JOURNAL OF MATERIALS SCIENCE 37 (2002) 2053–2059

The effects of C ion implantation on the near surface microstructure and properties of alpha alumina

M. E. MURPHY, M. T. LAUGIER*
Department of Physics, University of Limerick, Limerick, Ireland
E-mail: michael.laugier@ul.ie

B. D. BEAKE
Micro Materials Ltd, Wrexham Technology Park, Wrexham, UK

D. SUTTON, S. B. NEWCOMB*
Materials and Surface Science Institute, University of Limerick, Limerick, Ireland
E-mail: simon.newcomb@ul.ie

Biomedical grade (>99.5% purity) alpha-alumina has been implanted with carbon ions at fluences ranging from 5×10^{16} to 5×10^{17} C ions/cm^2 at an ion energy of 75 keV. The surfaces of the alumina have been examined in cross-section using transmission electron microscopy (TEM) and the data correlated with both nanohardness measurements and computer based simulations (Transport and Range of Ions in Matter, TRIM). TEM examination of the implanted surface has demonstrated the formation of a sub-surface amorphous layer as well as other microstructural modifications that are characteristic of ion damage. The nanohardness of the near-surface alumina was determined as a function of depth and was found to be strongly dependent on the fluence used.

1. Introduction

Ion implantation is a method by which the surface and near surface characteristics of materials can be modified whilst maintaining their bulk properties [1–3]. The physical changes induced by ion implantation are due to atomic and nuclear collisions, which can lead to the formation of highly disordered and eventually amorphous structures. Chemical changes can originate from the formation of precipitates [4] (resulting from the use of active ion species) or surface alloys [5] (resulting from the introduction of alloying elements). For metals and ceramics, such changes may involve solid solution formation, the accumulation of radiation damage with progressive structural degradation or even the formation of new phases [2]. The extent of this damage depends on six major ion implantation parameters: ion species, substrate species, beam energy, fluence, beam current density and substrate temperature [4].

Modification of the near-surface regions of alumina through ion implantation using different ions have been previously investigated [6–14]. A number of studies of the ion implantation of alumina (Al_2O_3) examined the effects of fluence and beam energy on the mechanical and chemical properties of the substrate [6–9]. McHargue, for example, has investigated the implantation of alumina with zirconium ions under doses ranging from 2×10^{16} Zr ions/cm^2 (150 keV) [4] to 2×10^{17} Zr ions/cm^2 (175 keV) [6]. Such studies have shown that Zr causes more damage per unit fluence by comparison with ions such as Cr [8] or Cu [10], a difference that has been attributed to the size of the Zr ion. An amorphous subsurface layer has been observed after implantation at a fluence of 4×10^{16} Zr ions/cm^2 (150 keV) whereas at a lower fluence of 2×10^{16} Zr ions/cm^2 (150 keV), the formation of an interstitial solid solution occurred. The thickness of this sub-surface layer was found to rise with increasing fluence and the surface mechanical properties were also found to be dependent on the fluence used. For a fluence of 2×10^{16} Zr ions/cm^2, the hardness of the surface of the alumina was found to increase by approximately 40% [4], whereas at a higher fluence (2×10^{17} Zr ions/cm^2), the hardness was some 60% lower than for an unimplanted sample [10, 11]. Further implantation studies on alumina have been reported with ions such as Cu [10, 12], Nb [6], Fe [6, 7], Y [2], Ni [13], Ar [14] and N [14] ions. In general, similar trends have been observed with the formation of a subsurface amorphous phase that increases in thickness with increasing fluence, whilst compressive residual stresses [2] are set-up in the surface.

Previous research has reported that the microstructural modification of alumina by C ion implantation

*Authors to whom all correspondence should be addressed.

improves the tribological performance through the formation of a graphite-like carbon structure at the surface layer of the alumina [15]. The aim of the study described here has been to examine the effects of carbon ion implantation on the near surface hardness of biomedical grade alumina. Nanohardness has been measured as a function of depth and implanted carbon ion dose and the results correlated with the changes in microstructure of the implanted alumina, again as a function of depth. Comparisons have been made between the microstructure of the alumina both before and after carbon ion implantation. A computer based simulation (TRIM) method has been used in order to provide a further correlation between the qualitative TEM results for the carbon ion distribution with depth and the quantitative simulations of these distributions.

2. Experimental methods

The surfaces of polycrystalline biomedical grade alpha-alumina (>99.5% purity) were prepared using standard biomedical grinding and polishing methods [16] giving an R_a (Arithmetic average roughness—the average area per unit length between the roughness profile and its mean line) value of <0.02 μm. Ion implantation was performed using monocharged carbon ions at a beam energy of 75 keV and four different implant doses ranging from 5×10^{16} to 5×10^{17} C ions/cm^2. The hardness of the implanted and unimplanted samples was measured using a NanoTest nanohardness tester (Micro Materials, Wrexham, UK). The nanohardness was determined using a method previously described by Oliver and Pharr [17] from a 20 cycle load-partial-unload indentation, see Fig. 1a. This method permits the elastic and plastic components of indentation to be separated and the hardness to be calculated at each step as a function of depth.

Samples for TEM were prepared using focused ion beam thinning techniques and examined in a JEOL 2000FX. A software simulation based on the Monte Carlo technique (TRIM [18]) was used to approximate the distribution and range of the implanted carbon ions. The ion depth and distribution simulations have been correlated with both the nanohardness and the TEM data.

3. Results and discussion

All implantation parameters—with the exception of the ion dose—were kept constant throughout the implantation of the biomedical grade alumina. Fig. 1b illustrates the nanohardness data obtained for the various carbon ion dosages. The hardness of the unimplanted alumina was found to increase with decreasing depths beneath the surface. This change is due to the presence of residual stresses [19, 20] as well as microstructural damage within the near surface region of the ceramic and originates from the prior grinding and polishing processes used. Fig. 1b further demonstrates that for any given implantation, the hardness of the alumina falls with decreasing penetration depth. Such a fall appears to be promoted at the higher ion doses, whilst increasing the ion dose resulted in a further drop in the near surface hardness. The hardness was found to decrease over an

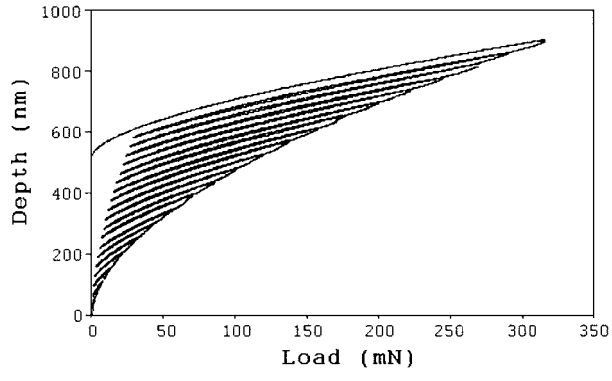

(a)

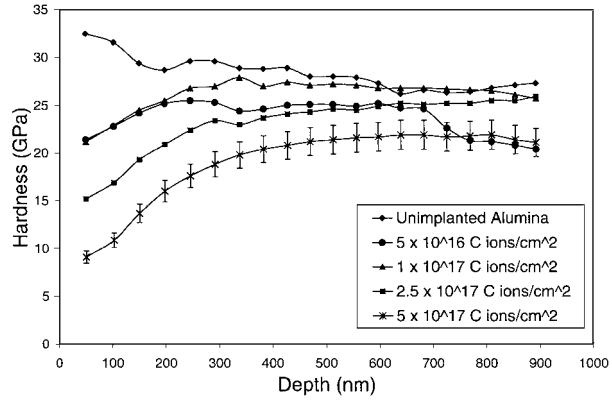

(b)

Figure 1 (a) A typical trace for a 20 cycle load partial-unload indentation from which nanohardness is determined as a function of depth; (b) The variations in nanohardness with depth for unimplanted alumina and alumina surfaces implanted at fluences of 5×10^{16}, 1×10^{17}, 2.5×10^{17} and 5×10^{17} C ions/cm^2.

increasing range beneath the surface with increasing ion dose. The result of this load partial-unload indentation reveals a dose dependant relationship for the carbon implanted alumina samples. From Fig. 1b, the near surface hardness—at depths less than 200 nm—can be seen to decrease with increasing carbon ion dose, particularly at the higher dosages. This relationship can be explained by the damage created to the crystal structure of the alumina by the implanted ions [21].

The ion induced microstructural damage was investigated through the TEM examination of the surface region of high dose (5×10^{17} C ions/cm^2) carbon implanted alumina as well as the unimplanted alumina so as to enable a comparison to be made. A typical region of the unimplanted surface of the alumina can be seen in the cross-sectional bright field image in Fig. 2a. The upper surface of the alumina has been capped by the Pt coating marked at A in order to prevent ion damage during the ion beam thinning preparation of the sample. The bulk of the underlying ceramic (as at B) was found to consist of equiaxed grains which varied in diameter from some 1.2 to 3 μm and to contain both intra- and inter-granular pores, as marked at C and D respectively. There was no evidence, however, that such porosity is of any significance in relation to the damage brought about by the implantation treatment described below. The upper region of the unimplanted alumina was examined in detail and it was found to consist of an irregular band (varying in depth from approximately 300 to 680 nm) of heavily dislocated grains, there being high

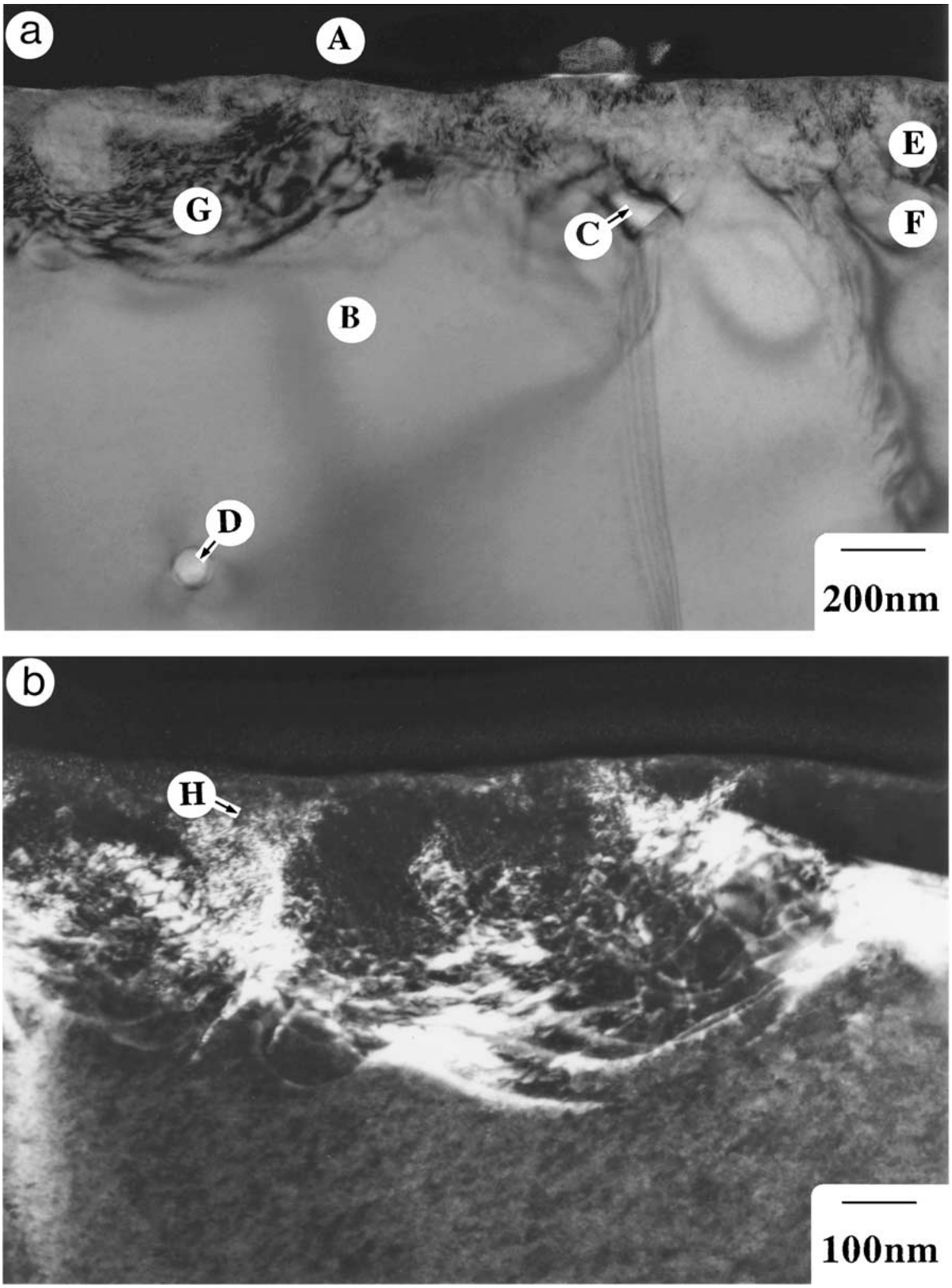

Figure 2 (a) Bright field and (b) higher magnification dark field micrographs showing the microstructures of a near-surface region of the unimplanted alumina.

misorientations between regions such as those marked at E and F. The area marked at G, in Fig. 2a, can be seen at higher magnification in the dark field micrograph shown in Fig. 2b which provides further evidence for the high dislocation content within the band lying at the surface of the alumina. It is also noted that there was a tendency for sub-grain boundary formation to occur at a depth of some 50–80 nm beneath the upper surface of the alumina, and this type of irregular boundary has been marked at H in Fig. 2b. The formation of such a highly dislocated band of alumina is likely to occur during the grinding and polishing treatments used prior to the ion implantation and appears to be consistent with the nanohardness data shown earlier in Fig. 1b for the unimplanted surface. Although it is recognised that annealing would reduce this type of mechanically

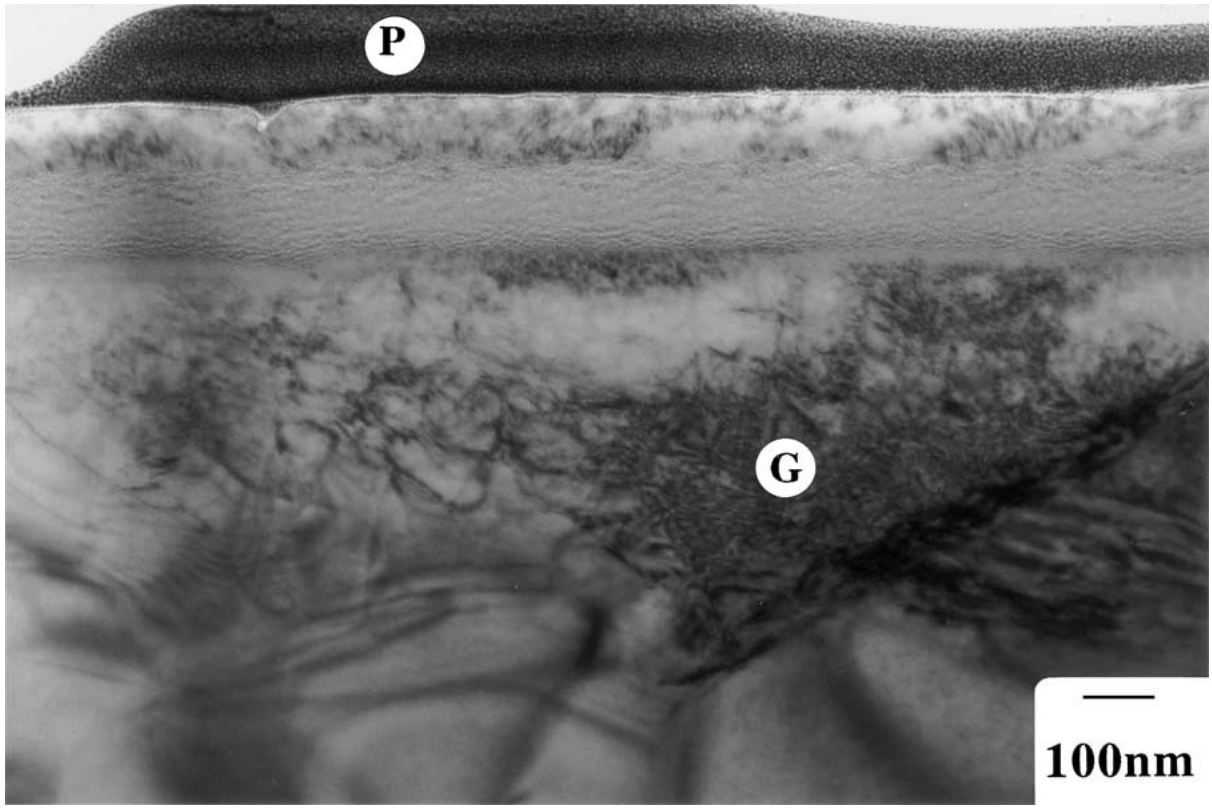

Figure 3 Bright field micrograph of a near-surface region of alumina implanted with carbon ions at a fluence of 5×10^{17} C ions/cm^2.

induced damage, the results described remain relevant to surfaces prepared for biomedical applications.

A cross-sectional bright field TEM micrograph of alumina implanted with carbon ions at 5×10^{17} C ions/cm^2 (75 keV) is shown in Fig. 3. The upper surface of the ceramic has again been coated with the protective high atomic layer marked at P. Part of the surface region in which a number of surface zones can be distinguished is shown at higher magnification in Fig. 4. Fig. 4a is a bright field micrograph which demonstrates the presence of a zone (as at A) immediately beneath the surface of the alumina and which extends to a depth

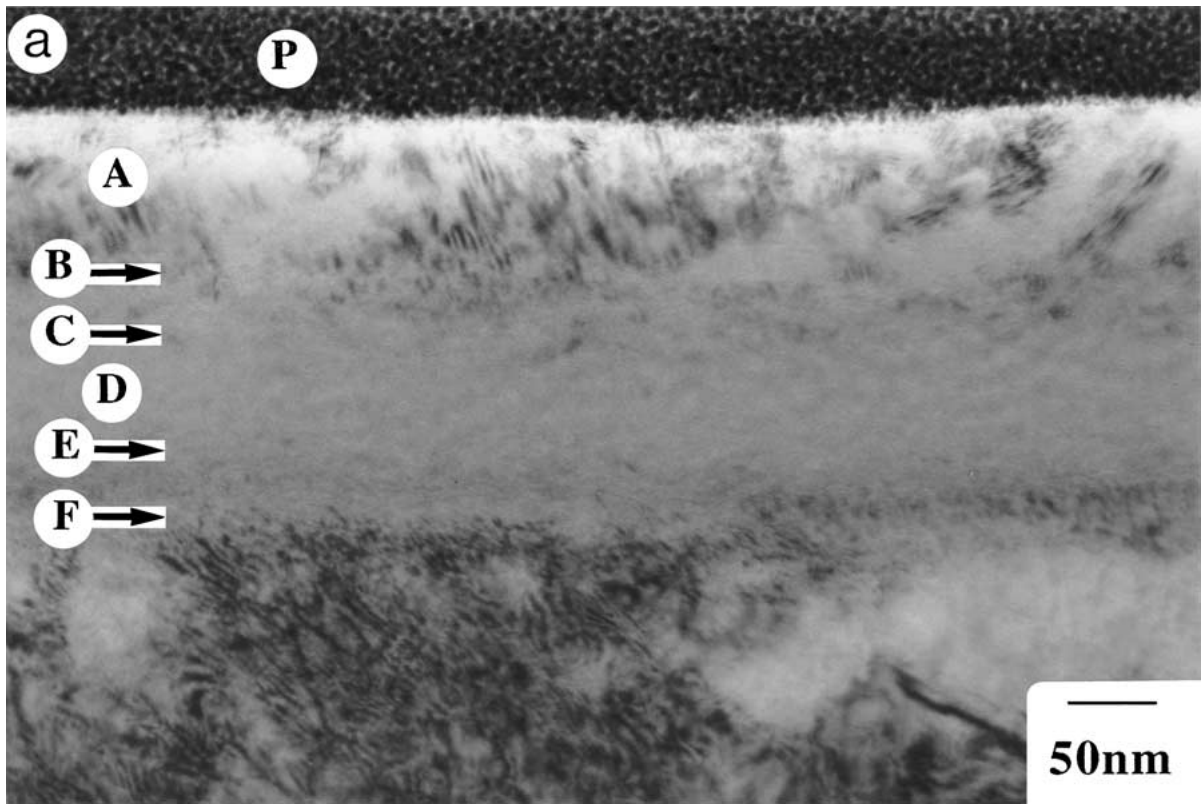

Figure 4 (a) Bright field and (b) dark field micrographs of the implanted alumina surface. The formation of different sub-layers is indicated by the regions marked at A–F. (*Continued.*)

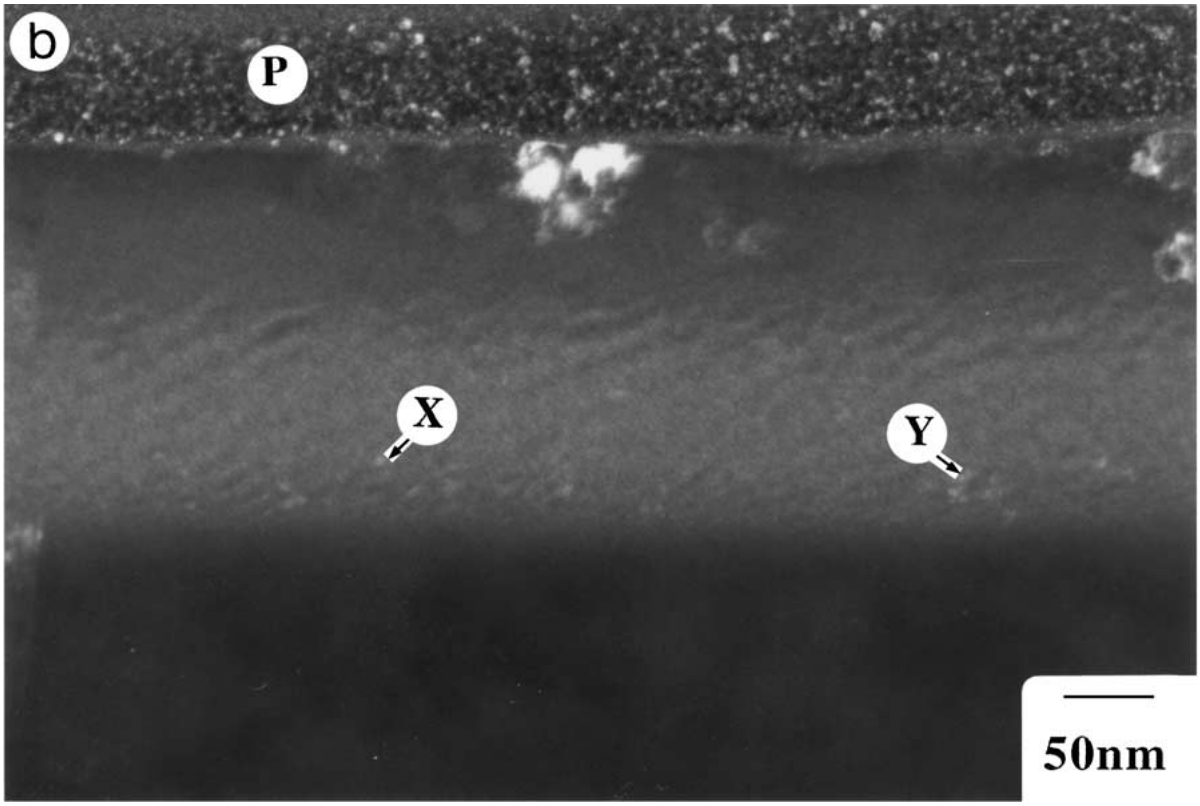

Figure 4 (*Continued.*)

of approximately 75 nm to the position marked at B. Comparison with the dark field image shown in Fig. 4b indicates that this part of the alumina is made up of reasonably fine equiaxed grains which have an approximate diameter of 50 nm and thus exhibit clear differences between the unimplanted surface. The bulk of the changes induced by ion implantation were seen in the formation of an amorphous layer (as at D) which extended from the base of the upper zone of equiaxed grains (as at B) to a depth of approximately 225 nm beneath the surface of the alumina, as indicated by the position marked at F in Fig. 4a. The disordered nature of this part of the structure is confirmed by the form of the objective aperture dependent speckle contrast seen in the dark field image shown in Fig. 4b. Fig. 4b is of further interest for the way in which the upper and lower parts of the amorphous zone were found to be interspersed with very fine equiaxed grains of alumina, which typically exhibited stringer morphologies. Examples of such grains, which have typical diameters of 5 nm, have been marked at X and Y in Fig. 4b and these amorphous/nanocrystalline zones were found to be located within the bands marked at B-C and E-F at distances of 75–125 nm and 185–225 nm respectively from the surface of the alumina.

A comparison can be made with the TRIM simulated distribution of implanted carbon ions (for a dose of 5×10^{17} C ions/cm^2) shown in Fig. 5. The maximum intensity for such ions can be seen to lie at a depth of some 140 nm beneath the surface of the alumina, the distribution of ions above and below this position being seen to exhibit a degree of asymmetry. Implantation can be seen not to have taken place at depths greater than approximately 225 nm whereas there is a distinct 'tail' in the C ion distribution towards the surface of the

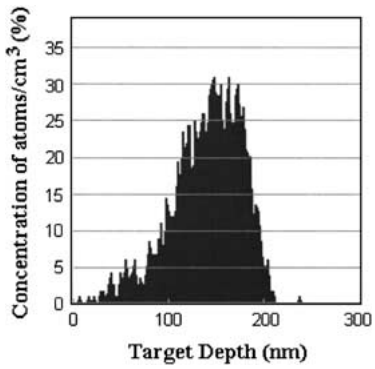

Figure 5 TRIM simulated distribution of implanted C ions for a dose of 5×10^{17} C ions/cm^2 as a function of depth.

alumina. The position of the maximum in the number of implanted C ions can thus be seen to lie at the centre of the amorphous zone described in Fig. 4a whilst the half-height peak-width positions lie very close indeed to the boundaries marked at C and E in Fig. 4a, above and below which the amorphous layer was found to be intermixed with very fine grains of alumina. The forward tail in the simulated C ion distribution appears to correspond to the zone containing the somewhat coarser 50 nm alumina grains within the band marked at A in Fig. 4a. The critical point, however, is the way in which there is such close correlation between the simulated C ion distribution and the position of the amorphous zone, the formation of which is likely to be related to the lattice damage created by the implanted C ions.

The microstructure of the alumina situated beneath the amorphous zone was similarly examined using TEM and significant differences were found between the same regions observed in the unimplanted surface. Whereas the latter exhibited the formation of an

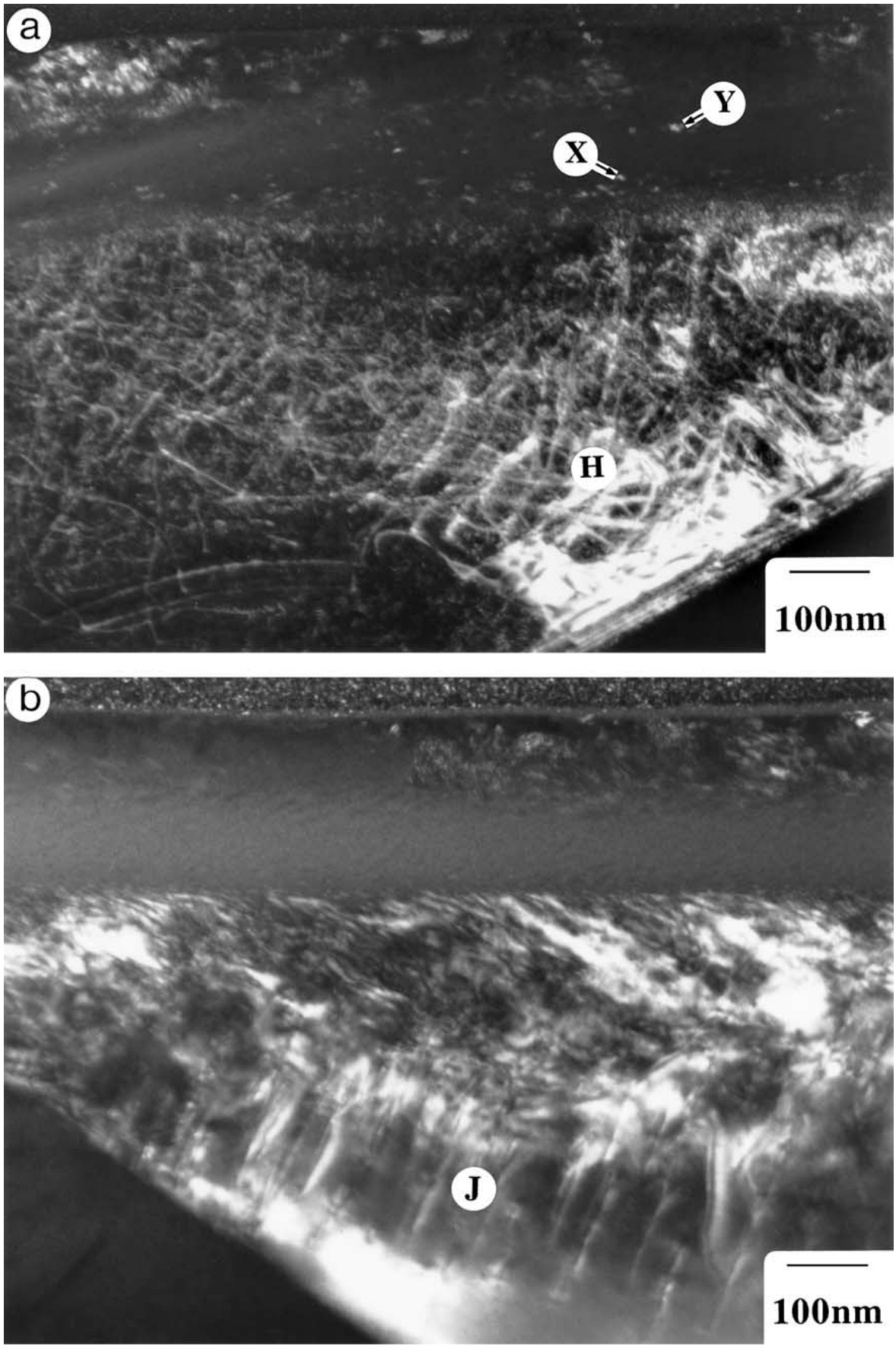

Figure 6 Dark field micrographs, (a) and (b), showing deformation of the alumina grains beneath the implanted zone.

irregular band of high dislocation content, which extended to depths of 300–680 nm beneath the surface of the alumina, here the region marked at G in Fig. 3 is somewhat more uniform but again contains a very high density of dislocations.

The high defect content of this part of the alumina is typified by the region marked at H in the dark field micrograph shown in Fig. 6a whilst a more regular array of dislocations can be seen to have been formed at J (in Fig. 6b). The latter type of defect was found at depths of

1 μm from the surface of the alumina and was present at much higher densities than in the unimplanted surface.

The increase in the localised defect density within the alumina situated beneath the near surface amorphous band implies that a compressive stress has been formed due to the presence of the implanted carbon ions. The formation of such a residual stress can be explained by the ensuing volume change [22] in the implanted region. If this volume change causes the implanted region to expand, a lateral residual stress will be produced due to the lattice expansion of the implanted region being restrained by the much larger underlying undamaged region of the substrate. For the surface described, some of the compressive stress has been relieved by the formation of dislocations within the unimplanted region.

4. Conclusions

The effects of carbon ion implantation on the surface hardness and microstructure of biomedical grade alpha alumina have been investigated using nanohardness and transmission electron microscopy. The near surface hardness was found to be dependent on the ion dosage used and tended to decrease with increasing carbon ion dose. The microstructures of unimplanted and high dose carbon implanted alumina have been investigated by TEM. It has been found that the microstructure of alumina is modified using high-dose carbon ion implantation, as demonstrated by the presence of an amorphous layer at a dose of 5×10^{17} C ions/cm^2. This amorphisation is apparently directly related to the reduction in the near surface hardness of the implanted alumina.

Acknowledgements

This study was financially supported by an Enterprise Ireland Strategic Research Grant, under Contract No. ST/98/423. We are grateful to Professors D. N. Buckley and B. K. Hodnett for the provision of laboratory facilities. We also thank Mr. Gerard Insley of Stryker Howmedica Osteonics, Limerick, Ireland for supplying the biomedical grade alumina.

References

1. S. A. DILLICH and D. BEIDERMAN, *Mat. Sci. and Eng.* **90** (1987) 91.
2. P. J. BURNETT and T. F. PAGE, *J. Mater. Sci.* **19** (1984) 3524.
3. G. B. STACHOWIAK, G. W. STACHOWIAK and P. EVANS, *Wear* **241** (2000) 220.
4. C. J. MCHARGUE and C. S. YUST, *J. Amer. Ceram. Soc.* **67** (1984) 117.
5. G. BATTAGLIN, *Nucl. Instrum. Meth.* B **116** (1996) 102.
6. C. J. MCHARGUE, *Mat. Sci. and Eng.* A **253** (1998) 94.
7. C. J. MCHARGUE, M. E. O'HERN, C. W. WHITE and M. B. LEWIS, *ibid.* **115** (1989) 361.
8. C. J. MCHARGUE, C. W. WHITE, B. R. APPLETON, G. C. FARLOW and J. M. WILLIAMS, *Mat. Res. Soc. Symp. Proc.* **27** (1984) 385.
9. L. BOUDOUKHA, S. PALETTO and G. FANTOZZI, *Nucl. Inst. and Meth.* B **108** (1996) 87.
10. *Idem.*, *J. Mater. Sci.* **32** (1997) 2911.
11. L. BOUDOUKHA, F. HALITIM, S. PALETTO and G. FANTOZZI, *Ceram. Int.* **24** (1998) 189.
12. F. HALITIM, N. IKHLEF, L. BOUDOUKHA and G. FANTOZZI, *Thin Solid Films* **300** (1997) 197.
13. T. HIOKI, A. ITOH, M. OHKUBO, S. NODA, H. DOI, J. KAWAMOTO and O. KAMIGAITO, *J. Mater. Sci.* **21** (1986) 1321.
14. T. HIOKI, A. ITOH, S. NODA, H. DOI, J. KAWAMOTO and O. KAMIGAITO, *ibid.* **3** (1984) 1099.
15. T. JUN, W. QIZU and X. QUNJI, *Nucl. Inst. and Meth.* B **143** (1998) 488.
16. E. SMETHURST and R. B. WATERHOUSE, *J. of Mat. Sci.* **12** (1977) 1781.
17. W. C. OLIVER and G. M. PHARR, *J. Mat. Res.* **7** (1992) 1564.
18. J. F. ZIEGLER, J. P. BIERSACK and U. LITTMARK, "The Stopping and Range of Ions in Solids" (Pergamon, New York, 1985).
19. B. J. INKSON, *Acta Mater.* **48** (2000) 1883.
20. L. PRANEVICIUS, K. F. BADAWI, N. DURAND, J. DELAFORD and P. GOUDEAU, *Surf. Coatings Technol.* **71** (1995) 254.
21. F. HALITIM, N. IKHLEF, S. ABDESLAM and G. FANTOZZI, *Ceram. Int.* **23** (1997) 509.
22. A. MISRA, S. FAYEULLE, H. KUNG, T. E. MITCHELL and M. NASTASI, *Nucl. Instrum. Meth.* B **148** (1999) 211.

Received 8 March 2001
and accepted 30 January 2002